

Experimental Study of the Performance of Bare and Nozzle – Diffuser Shrouded Micro Wind Turbine under axial and non-axial Inflow Condition

P.B. Kosasih¹, N. Bryce¹, A. Tondelli¹ and A. Beazley¹

¹School of Mechanical, Materials and Mechatronics Engineering
 University of Wollongong, New South Wales 2500, Australia

Abstract

Shrouding (*diffuser augmented*) horizontal axis micro-wind turbine has been shown to be an effective ways to improve the performance of micro wind turbine. The paper reports experimental work on the effects of shroud/diffuser shape and geometry on the turbine performance. Three different diffuser shapes: straight diffuser, nozzle-diffuser combination, and diffuser-brim (*brimmed diffuser*) combination have been investigated. Tests confirmed that placing micro wind turbine model inside a diffuser can substantially improve its performance. Straight diffuser improves the performance by 56% compared to the bare turbine whilst the nozzle-diffuser enhancement of 61% is slightly better than diffuser only. Increasing the diffuser length does not improve the turbine performance but adding brim at the exit plane of the diffuser does. The effect of non-axial inflow on the model wind turbine was also investigated. Non-axial inflow decreases the coefficient of performance of the turbine. The finding from this work demonstrates that shrouding micro wind turbine not only improves the performance but also demonstrates how diffuser geometrical features diffuser length, brim height and nozzle addition can be used to design high performance turbine to suit wind condition at location. Further testings and optimisations could lead to the realisation of optimal augmentation for micro wind turbine, which would have great implications for wind power extraction in built environment.

Introduction

Diffuser-augmented wind turbine has been shown by many studies [1-4] can significantly increase power output. Simple diffuser consists of three sections (Figure 1a): inlet section, turbine section or throat, and diffusing outlet section. The overall performance augmentation depends on the design of each section and governed by the efficiencies of the inlet and outlet sections, the static pressure at the outlet area of the diffuser, and the resistance from the turbine [5]. For simple design as shown in Fig. 1, parameters that influence the performance include length, l and angle, γ of the inlet section, and length, L and expansion angle, α of the diffuser. Despite of the importance of diffuser geometrical parameters there is limited experimental study comparing the performance of the bare turbine with shrouded turbine under controlled flow condition and rotor speed.

Matsushima *et al.* [6] studied the effect of diffuser length, L , expansion angle, α and brim height on the increase of wind speed under unloaded condition (*no turbine*) at the throat. L/D from around 0.4 to 3 was investigated. van Bussel [4] using simple momentum theory reached the same finding *i.e.* proportional increase of coefficient of performance, C_p with diffuser area ratio. On the other hand increasing α initially increases wind speed ratio but after reaching the maximum, the ratio decreases indicating the occurrence of detached flow inside the diffuser.

The main performance augmentation has been shown to be the result of the sub-atmospheric pressure condition at the diffuser exit plane allowing more air to flow into the turbine and more energy extracted from the wind [1,2]. The increase of C_p is shown proportional to the increase in ratio of mass flow through the turbine in the diffuser and through the bare turbine [3]. If the diffuser has aerofoil shaped cross-section more air will pass through the diffuser.

Ohya *et al.* [7] showed that with the addition of broad ring flange (*brim*) in the outlet of the diffuser the pressure at the exit plane can be lowered further due to the vortex formation at the outlet plane. Hence performance of brimmed diffuser shrouded turbine is greater compared to diffuser only. Compared to same diffuser without brim, the flow must expand to lower pressure. As the expansion in the brimmed diffuser and non-brimmed one is the same, the pressure downstream of the brimmed diffuser turbine must be lower and hence flow is accelerated [8].

Another mechanism was also identified by Abe *et al.* [9] who observed the affected flow structure behind the turbine particularly near the blade tip [9]. The presence of the diffuser wall suppress the separation region hence increase the power output of the turbine. This is more evident at low tip speed.

The paper presents performance comparison of bare and diffuser-augmented/shrouded (diffuser only, nozzle-diffuser and diffuser-brim shroud) micro wind turbine. The experiment carried out in this work is different from the previous reported experiment in several aspects including: controlled experimental conditions *e.g.* tip speed ratio, λ , direct measurement of power output, and subject to axial and non-axial inflow condition.

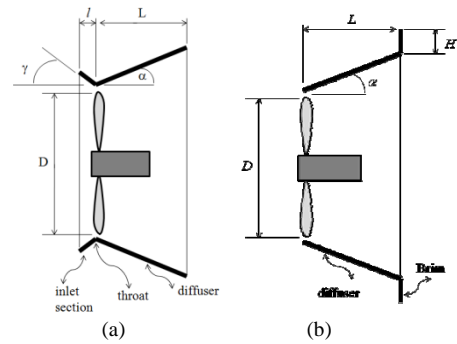


Figure 1. Simple shroud designs for wind turbine: (a) nozzle-diffuser and (b) diffuser-brim shroud.

Experimental Micro Wind Turbine Model

The rig was designed with detachable diffuser allowing comparison of bare turbine against shrouded turbine with minimum variations other than the diffuser attachment. Figures 2 show the turbine with straight diffuser attached (a) and (b) with nozzle-diffuser.

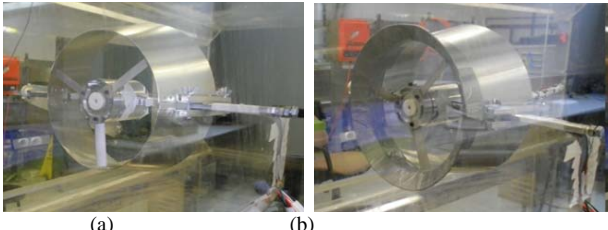


Figure 2. Wind Turbine mounted in wind tunnel test section (a) diffuser - augmented turbine; (b) nozzle – diffuser augmented turbine set-up.

The model turbine has three blades. The blades have NACA 63-210 airfoil profile. The rotor diameter is 190mm. The tip gap is kept as small as practically possible *i.e.* 2-3mm. The diffuser length is 120mm resulting in L/D of 0.63. The diffuser expansion angle, α is 12° giving diffuser outlet and inlet area ratio of 1.61. The major dimensions of the ducted wind turbine model are given in Table 1. The turbine was placed in a wind tunnel with working section of 450mm x 450mm x 1500mm and wind speed up to 25ms^{-1} .

	Dimension	Value	Units
Nozzle	Inlet diameter	244	mm
	Outlet diameter	190	mm
	Length	33	mm
	Opening angle (γ)	45	degrees
Diffuser	Rotor diameter (D)	190	mm
	Outlet diameter	240.73	mm
	Length (L)	120	mm
	Expansion angle (α)	12	degrees
Hub	Diameter	62	mm
	Length	95	mm
Blade	Span	64	mm
	Chord	25	mm
	Thickness	2.5	mm
	Number	3	

Table 1. Major dimensions of the shrouded wind turbine model.

The wind energy conversion into mechanical power was directly measured from the torque and rpm measurements. The torque measurement system was designed following method introduced by Gluskin [10]. In this case, the torque measured is the torque applied directly to the motor stator. The reaction forces that oppose the electromagnetic torque create an equal and opposite torque that is applied to the stator. A link rod connected to a load cell can provide a means of measuring this torque exerted on the stator, as depicted in Figure 3. The torque measurement system was calibrated with static loading. The calibration was found to be linear within the tested range -600 - + 600 grams.

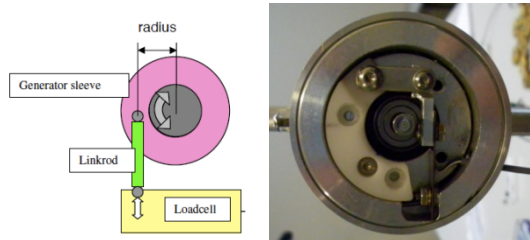


Figure 3: Method of measuring torque on the motor stator by using a linkrod connected to a load cell.

The turbine is attached to a DC 120 Watt Maxon motor with matching motor controller (4-q-EC Servo amplifier DES70/10). The rotational speed of the rotor can be precisely controlled. As the wind flow over the blades the induced lift produces torque that turns the stator. The free stream wind through the test tunnel section was measured and monitored by an anemometer.

Due to the size of the turbine diameter of 190mm, the maximum practically attainable tip speed ratio, λ is 2.5 for the bare turbine

case and 3.5 for the diffuser-augmented turbine. The experimental procedure is as follows. The wind speed to induce 2500rpm free spinning of the rotor was initially determined. It was found that 10ms^{-1} and 7ms^{-1} were the required wind speed to spin the rotor at 2500rpm under no load other than motor resistive load for bare turbine and DAWT respectively. Once these wind speeds had been found, the speed was maintained constant. The rpm of the rotor was then controlled but must be below 2500rpm. Thus the variation of λ is achieved by varying rpm at the chosen wind speeds. The power capture by the turbine is given by the torque measured by the load cell multiplied by the rotor rpm registered by the controller. C_p is given by the definition

$$C_p = \frac{T\omega}{0.5\rho AU^3} \quad (1)$$

In the case of bare turbine A is the turbine swept area whilst in the case of diffuser augmented turbine A is the diffuser outlet area. The power measurement is important in this experiment and effort was made to ensure the accurate torque measurement was achieved. As has been shown the load cell voltage and load relation was linear, so the tests were operated in the linear regime and the under steady state wind condition. In this condition the torque should be constant, however during the experiment fluctuating torque was sensed when the rotor was operated at closed to certain rpm perhaps close to the resonant frequency of the set-up. So tests were conducted with the settings at which vibration did not cause any torque fluctuations.

Results and Discussion

Bare Turbine Performances

The relationship between C_p and λ (from 0.5 to 2.5) for the bare micro wind turbine for various inflow angles (0° , 5° , 10° and 15°) is shown in Figure 4. The data plotted in the figure is the mean data. C_p reaches a maximum value at an optimal λ . This phenomenon is explained below. As λ increases the relative wind speed seen by the turbine blades increases and becomes more parallel to the blade chord. This causes an increased flow over the blade and consequently greater lift force produces greater torque on the motor stator resulting in greater coefficient of performance. This process repeats until the rotational speed of the blades becomes too high that the wind sees the turbine blades as a blockage and predominantly flow around the outside of the turbine rather than through it. The inflow angle affects a slight decrease in C_p and shift toward lower λ as the inflow angle is increased. This occurrence is due to a reduction in the projected swept area and a reduction in the flow component perpendicular to the rotor [11].

It is difficult to compare the bare turbine results obtained here with published literature as there are numerous factors that influence a bare turbine's performance including blade profile; blade diameter, swept area, as well as the number of blades used that are not the same with the tests' conditions. It is of more relevance to obtain the percentage increase in C_p of the same turbine with different shrouds (diffuser and nozzle-diffuser) and compare this value to published literature. Kishinami *et al.* [12] have experimentally obtained coefficient of performance versus tip speed ratio curves of bare turbines with maximum C_p between 0.3 and 0.4 was observed. These values are similar to the experimental values obtained in this work, and although a direct comparison between turbines cannot be made, this previous literature significantly enhances the validity of the results obtained and the experimental technique done in this work. The optimal tip speed ratio in this literature, however, is found to

occur at four to five rather than the experimentally obtained value of two here. This can be attributed to the use of larger turbines *i.e.* 1000mm in [12], which require higher tip speed ratios for the turbine blades to see a similar relative velocity (U_{rel}) as seen by our micro wind turbine at a tip speed ratio of two (as R increases, ω decreases for the same tip speed ratio).

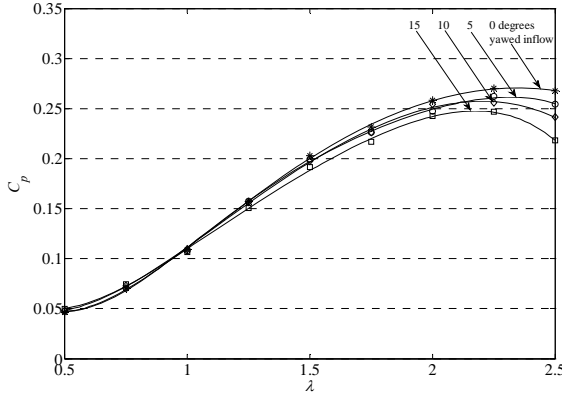


Figure 4. C_p vs. λ (bare turbine with 0° - 15° non-axial inflow angle). For 0° the maximum C_p is 0.27 and the optimum λ is 2.3. For 5° the maximum C_p is 0.263 and the optimum λ is 2.25. For 10° the maximum C_p is 0.256 and the optimum λ is 2.2. For 15° the maximum C_p is 0.247 and the optimum λ is 2.15.

Pederson [11] prediction (Eq. 2) of performance under non-axial inflow matches well with experimental values.

$$C_p = C_{p@0^\circ} \cos^2 \Phi \quad (2)$$

where Φ is the non-axial inflow angle. The results obtained in this experiment are also consistent with that of Maeda *et al.* [13], who have also shown experimentally that the optimal tip speed ratio decreases with increasing yaw angle.

Diffuser Augmented Turbine Performances

The relationship between C_p and λ (ranging from 0.5 to 2.5) for the diffuser shrouded micro wind turbine, under various inflow angles (0° , 5° , 10° and 15°) is shown in Figure 5. Unlike the C_p calculations in the bare turbine case, the swept area, A for the shrouded wind turbine is taken as the outlet area of the diffuser rather than the swept area of the turbine blades.

C_p increases with increasing λ until it reaches a maximum value, after which it begins to decline. The maximum C_p and λ , however, are much higher when compared to that of the bare turbine and this phenomenon is explained as follow. As outlined in the introduction vortices at the exit of the diffuser create low pressure systems which draw more air, at a higher speed, through the inlet and consequently through the plane of the turbine blades. This creates a higher relative velocity (U_{rel}) seen by the turbine blades than in the bare turbine experiments for the same tip speed ratio, which increases the torque exerted on the motor stator and therefore explains the increase in C_p . The presence of this low pressure system also draws air through the turbine blades at higher tip speed ratios than in the bare case, hence further increasing the relative velocity (U_{rel}) seen by the turbine blades creating a higher maximum coefficient of performance and higher optimal tip speed ratio. The maximum coefficient of performance was shown to increase by 56% from 0.27 to 0.42 by using the diffuser augmentation, hence showing a clear advantage in the use of these devices over bare turbines for wind power extraction.

The effect of non-axial inflow, however, on the performance of the diffuser augmented wind turbine is significantly greater than

that of the bare turbine. Increasing the non-axial inflow angle was found to decrease the maximum coefficient of performance and optimal tip speed ratio dramatically. This effect can be attributed to: similar to the effect of non-axial inflow on the bare turbine *i.e.* with increasing inflow angle the projected swept area and flow component perpendicular to the rotor are reduced, thus reducing the torque exerted on the motor stator. With increasing angle, the diffuser itself provides easy passage for wind to flow around it by bouncing off the angled sides of its body, which significantly reduces the intensity of the low pressure system at the exit of the diffuser. This causes significant reduction in the flow of air drawn through the diffuser inlet, and a reduction in the speed of the flow. Consequently the maximum coefficient of performance and optimal tip speed ratio are dramatically reduced even with small increases in non-axial inflow angle.

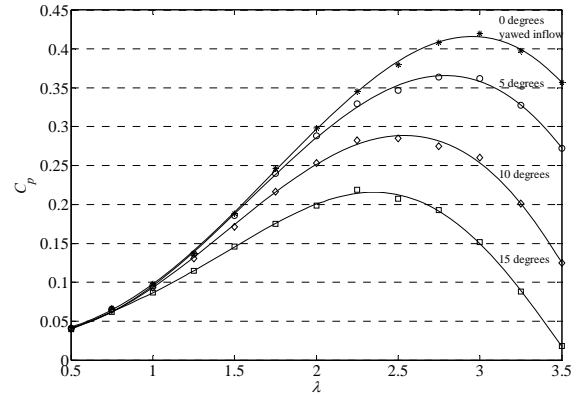


Figure 5. C_p vs. λ (diffuser augmented turbine with 0° - 15° non-axial inflow angle). For 0° the maximum C_p is 0.42 and the optimum λ is 3. For 5° the maximum C_p is 0.364 and the optimum λ is 2.75. For 10° the maximum C_p is 0.285 and the optimum λ is 2.5. For 15° the maximum C_p is 0.219 and the optimum λ is 2.25.

Nozzle-Diffuser Augmented Turbine Performances

The relationship between Coefficient of Performance and Tip Speed Ratio (ranging from 0.5 to 2.5) for the nozzle-diffuser augmented micro wind turbine, under various inflow angles (0° , 5° , 10° and 15°) is shown in Figure 6.

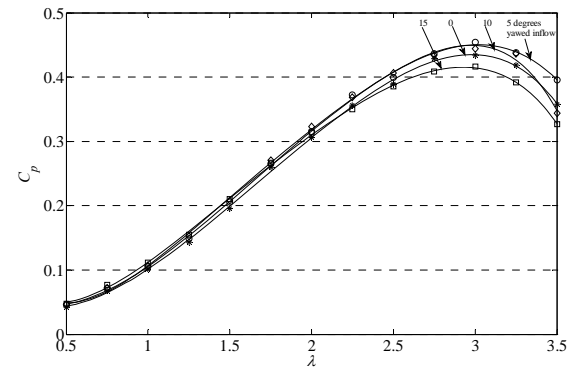


Figure 6. C_p vs. λ (nozzle-diffuser augmented turbine with 0° - 15° non-axial inflow angle). For 0° the maximum C_p is 0.434 and the optimum λ is 3. For 5° the maximum C_p is 0.454 and the optimum λ is 3. For 10° the maximum C_p is 0.444 and the optimum λ is 3. For 15° the maximum C_p is 0.417 and the optimum λ is 3.

The performance of the nozzle-diffuser augmented wind turbine under 0° yaw angle shows a slight increase of 1.7% in maximum coefficient of performance when compared to that of the diffuser only augmented turbine (same optimal λ). This is due to the nozzle essentially capturing a larger frontal area of wind and

consequently increasing the mass flow of air through the turbine blades. The actual diffuser section of this augmentation has not changed and therefore the intensity of the vortices and the low pressure system at the exit is not significantly increased. This explains the only slight increase in maximum coefficient of performance. Nonetheless, the addition of the nozzle increased the coefficient of performance by approximately 61% (from 0.27 to 0.434) when compared to the bare turbine.

The performance of the nozzle-diffuser augmentation, under increasing non-axial inflow, is significantly better than the diffuser augmentation. This is due to: the addition of the nozzle to the front of the diffuser makes it much more difficult for air to flow around the augmentation up to 15° inflow angle. This keeps a close to constant flow of air through the diffuser inlet and thus the intensity of the low pressure system at the exit remains relatively constant. This causes a similar relative velocity (U_{rel}) to be seen by the turbine blades with increasing non-axial airflow, resulting in similar torques and consequently similar power to be extracted by the turbine at increasing non-axial inflow angles. The performance under non-axial inflow is relatively constant for angles between $0 - 10^\circ$ and it is not until 15° that significant performance reduction was observed. It is predicted that performance would slightly decrease with increasing inflow angles due to a reduction in the projected frontal area and flow perpendicular to the rotor, however performance slightly increased above 0° for angles between 5° and 10° .

Nozzle-Diffuser-Brim Augmented Turbine Performances

The next parametric study looks at the effect of the brim height (H/D). The effect of increasing the brim height is illustrated in Fig. 7. Increasing H/D increases both C_p and shift λ at which the optimum C_p occurs towards higher λ . These phenomena may be explained as follow. The brim causes vortices to appear at the exit of the diffuser [3]. The vortices increase the kinetic energy at the exit region and induce sub-atmospheric back pressure *i.e.* lowering C_{pe} , which results in increased mass flow rate for a given free stream wind speed. Wind speed is increased at the rotor plane with increasing H . Because of this the rotor must spin faster to capture the wind energy hence shifting λ toward higher value.

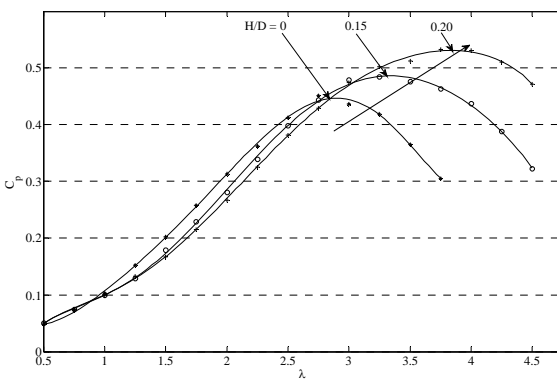


Figure 7. The effect of H/D on the performance comparison of brimmed diffuser shrouded micro wind-turbine.

Conclusions

C_p of the micro wind turbine increased by approximately 56% with the addition of simple conical diffuser, and 61% with the addition of nozzle-conical diffuser shroud compared to the performance of the bare turbine. The nozzle-diffuser augmentation was found to exhibit only slightly superior performance compared to the diffuser augmented *i.e.* only 5% compared to the diffuser augmented turbine. However contrary to

the diffuser only, the nozzle-diffuser augmentation hold its performance very well under non-axial inflow with only slight decreases in C_p . Diffuser length and brim height can affect the performance augmentation of a micro-wind turbine. Brim height can shift the performance curve toward higher λ as well as increase the optimum C_p . This demonstrates that shrouding micro wind turbine, albeit in the present work we only considered straight conical diffuser, not only improves its performance but also points out how diffuser geometrical features (L/D) and/or (H/D) can be used to design a turbine with performance curve to suit the location.

Acknowledgments

The authors acknowledge the financial support from the 2012 UoW URC small grant in this project.

References

- [1] Foreman, K.M., Gilbert B. & Oman R.A., Diffuser Augmentation of Wind Turbines, *Solar Energy*, **20**, 1978 305-311.
- [2] Igra O., Research and Development for Shrouded Wind Turbines, *Energy Conv. & Mgmt.*, **21**, 1981, 13-48.
- [3] Hansen M. O. L., Sorensen N. N. & Flay R. G. J., Effect of Placing a Diffuser around a Wind Turbine, *Wind Energy*, **3**, 2000, 207-213.
- [4] van Bussel G. J. W., The Science of Making More Torque from Wind: Diffuser Experiments and Theory Revisited, *Journal of Physics: Conference Series*, **75**, 2007, 1-12.
- [5] Lawn C. J., Optimization of the Power Output from Ducted Turbines, *Proc. Instn. Mech. Engrs. Part. A: J. Power and Energy*, **217**, 2003, 107-117.
- [6] Matsushima T., Takagi S. & Murayama S., Characteristics of a Highly Efficient Propeller Type Small Wind Turbine with a Diffuser, *Renewable Energy*, **31**, 2006, 1343-1354.
- [7] Ohya Y., Karasudani T., Sakurai A., Abe K. & Inoue M., Development of a Shrouded Wind Turbine with a Flanged Diffuser, *J. Wind Eng. and Industrial Aero.*, 2008, 524-539.
- [8] Abe K. & Ohya Y., An Investigation of Flow Fields around Flanged Diffusers Using CFD, *J. Wind Eng. and Industrial Aero.*, **92**, 2004, 315-330.
- [9] Abe K., Nishida M., Sakurai A., Ohya Y., Kihara H., Wada E. & Sato K., Experimental and Numerical Investigations of Flow Fields behind a Small Wind Turbine with a Flanged Diffuser, *J. Wind Eng. and Industrial Aero.*, **93**, 2005, 951 – 970.
- [10] Gluskin E., Possible Way to Measure the Mechanical Torque Developed by an Electric Motor, *European Journal of Physics*, **19**, 1998, 93.
- [11] Pederson T.F., On Wind Turbine Power Performance Measurements at Inclined Airflow, *Wind Energy*, **7**, 2004, 163-176.
- [12] Kishinami K., Taniguchi H., Suzuki J., Isono H., Kazunori T. & Turuhami M., Theoretical and experimental study on the aerodynamic characteristics of a horizontal axis wind turbine, *Energy*, **30**, 2005, 2089-2100.
- [13] Maeda T., Kurimamachi T., Kamada Y., Suzuki J. & Fujioka H., Rotor blade sectional performance under non-axial inflow conditions, *Journal of Solar Energy Engineering, Transactions of the ASME*, **130**, 2008, 0310181-0310187.